Nanotechnology **20** (2009) 235302 (6pp) doi:10.1088/0957-4484/20/23/235302

A well-ordered flower-like gold nanostructure for integrated sensors via surface-enhanced Raman scattering

Ju-Hyun Kim[1], Taejoon Kang[2], Seung Min Yoo[3], Sang Yup Lee[3], Bongsoo Kim[2,4] and Yang-Kyu Choi[1,4]

[1] Nano-Oriented Bio-Electronics Lab, Division of Electrical Engineering, School of Electrical Engineering and Computer Science, KAIST, Daejeon 305-701, Korea
[2] Department of Chemistry, KAIST, Daejeon 305-701, Korea
[3] Department of Chemical and Biomolecular Engineering, KAIST, Daejeon 305-701, Korea

E-mail: ykchoi@ee.kaist.ac.kr and bongsoo@kaist.ac.kr

Received 28 January 2009, in final form 6 March 2009
Published 18 May 2009
Online at stacks.iop.org/Nano/20/235302

Abstract
A controllable flower-like Au nanostructure array for surface-enhanced Raman scattering (SERS) was fabricated using the combined technique of the top-down approach of conventional photolithography and the bottom-up approach of electrodeposition. Au nanostructures with a mean roughness ranging from 5.1 to 49.6 nm were obtained by adjusting electrodeposition time from 2 to 60 min. The rougher Au nanostructure provides higher SERS enhancement, while the highest SERS intensity obtained with the Au nanostructure is 29 times stronger than the lowest intensity. The SERS spectra of brilliant cresyl blue (BCB), benzenethiol (BT), adenine and DNA were observed from the Au nanostructure.

(Some figures in this article are in colour only in the electronic version)

1. Introduction

Metal nanostructures and nanoparticles have been investigated intensively for various applications due to their electrical, optical, catalytic and biosensing properties [1–4]. The morphology of metal nanostructures has a particularly remarkable effect on the application of surface-enhanced Raman scattering (SERS) combined with the strongly localized surface-plasmon resonance characteristics of gold [5–8] and silver [9–12]. Although it is known that silver shows better SERS enhancement, gold is also favored as an SERS template due to its chemical stability and compatibility with various target molecules and buffer solutions during sample preparation [13].

To utilize metal nanostructures as SERS-active substrates, numerous techniques are feasible, such as e-beam lithography, nanosphere lithography, chemical aggregation of nanoparticles and oxygen plasma treatment [14–18]. While e-beam lithography is a typical top-down strategy for nanoscale patterning, it is severely time-consuming and provides low throughput in spite of its high level of precision in pattern sizing and positioning on a large substrate. In contrast, the bottom-up processes of chemical aggregation and self-assembly have advantages in terms of throughput and time effectiveness. Bottom-up techniques, however, continue to be associated with a lack of control in the positioning and patterning of the target materials. Hence, it is difficult to integrate all functional blocks into a system such as a lab-on-a-chip to satisfy the practical and specific demands of end-users. Thus, it is essential to develop a new approach that contains only the merits and eliminates the disadvantages of the aforementioned techniques.

In this study, a combined method of a top-down and a bottom-up technique is proposed to overcome the limits of previous approaches for a nanostructured template. The proposed nanofabrication process consists of two steps: lithography and electrodeposition. Photolithography on an Au film defines the size and position of a target nanostructure on a wafer-scale substrate with the high accuracy of a computer-aided design (CAD) tool, whereas the electrodeposition of $HAuCl_4$ on the patterned Au film provides a time- and cost-effective synthetic method of creating a nanoscale flower-like

[4] Authors to whom any correspondence should be addressed.

Au structure without a lithographic resolution limit. As a result, a well-ordered flower-like Au nanostructured array is fabricated on a silicon wafer. The SERS signal dependence on the surface morphology of the flower-like Au nanostructures is investigated and several diverse molecules, in this case brilliant cresyl blue (BCB), benzenethiol (BT) and adenine monomer, are detected with high sensitivity.

2. Experiment

2.1. Au micropattern fabrication

A schematic of the fabrication method of the flower-like Au nanostructure array is illustrated in figure 1(a). As a starting substrate, an Au film at a thickness of 100 nm was deposited by thermal evaporation onto a (100) silicon wafer after the deposition of a 10 nm thick Cr layer, which improves the adhesion of the Au film to the silicon. Subsequently, photolithography and etching defined the micropatterns of Au on the designated area to provide a seeding spot for the *in situ* electrodeposition. The micropatterns of photoresist were defined by optical photolithography using G-line ultraviolet light with a wavelength of 436 nm and an AZ6612KE positive photoresist. The photoresist patterns were used as an etching stopper for a subsequent Au/Cr wet etching process. In order to transfer the photoresist patterns to the Au layer, a 1:100 diluted KCN solution was used as a wet etchant. The wet etching process was performed at 25 °C for 60 s. After the etching process of the Au layer, the remaining Cr layer was etched by a CR-7 Cr etchant at 25 °C for 30 s. Finally, the remaining PR patterns were removed by AZ400T, the PR remover. As a result, the Au pattern array was fabricated on the silicon wafer which was used for an intentionally designed template of nanostructure synthesis.

2.2. Synthesis of flower-like Au nanostructure

Flower-like nanomicrocomplexes were formed onto a pre-patterned Au array via an electrodeposition (chemical synthesis) technique in an aqueous solution of $HAuCl_4$ and polyvinylpyrrolidone (PVP). After being cleaned with acetone and deionized water, the Au patterned wafer served as a working electrode and a graphite sheet was used as a counter electrode. DC voltage was applied to two electrodes immersed in the aqueous solution. Flower-like Au nanostructures started to grow and thereafter were crystallized on the pre-patterned Au microarray. Here, the geometric characteristics of the flower-like Au nanostructures depended on the concentration of $HAuCl_4$ and PVP, the applied voltage of the power supply and the electrodeposition time [19].

2.3. Measurement of SERS spectra

SERS spectra from flower-like Au nanostructures were obtained with a micro-Raman system based on an Olympus BX41 microscope. The 633 nm radiation of an He–Ne laser (Melles Griot) was used as an excitation source and the laser light was focused onto a sample through a 100× objective (Mitutoyo). The SERS signal was recorded with a thermoelectrically cooled electron multiplying charge-coupled device (EMCCD, Andor) mounted on the spectrometer with a 1200 groove mm^{-1} grating. A holographic notch filter was used to reject the laser light.

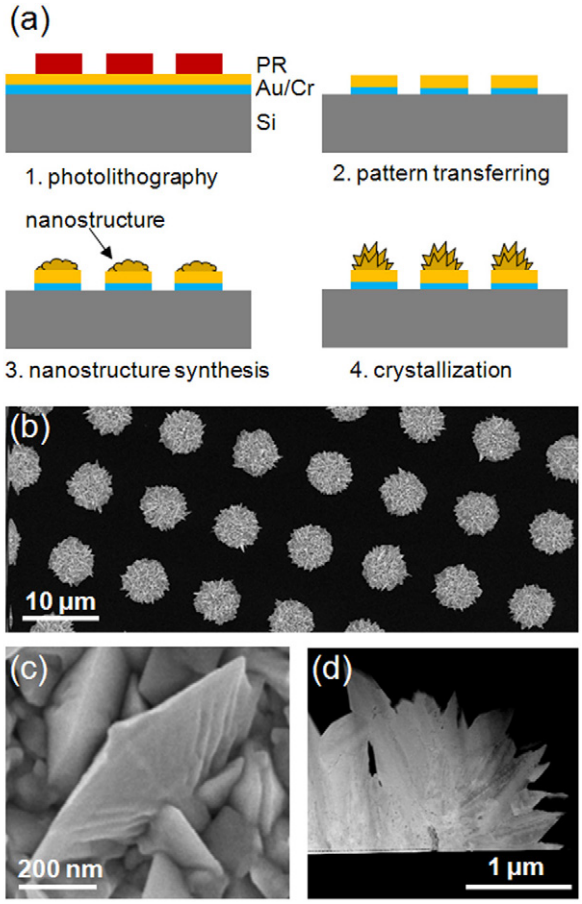

Figure 1. (a) Fabrication procedure of the flower-like Au nanostructure array: a conventional lithography and etching technique was combined with a bottom-up electrodeposition technique for Au nanostructures. (b) SEM image of the flower-like Au nanostructure array and (c) high magnification view of leaf-like Au nanoflake. (d) TEM image of a cross section of the single Au nanostructure.

3. Results and discussion

The scanning electron microscope (SEM) and transmission electron microscope (TEM) images in figures 1(b)–(d) show the well-ordered Au nanostructure array fabricated by the combined technique of top-down lithography and bottom-up electrodeposition. The flower-like Au nanostructure consists of numerous leaf-like Au nanoflakes, which resemble a vein of natural leaves (figure 1(c)). In other words, the facet of the nanoflake is not smooth like the well-deposited Au film. It has quite detailed and unique patterns on the surface like natural leaves. With the aid of this combinational approach, the nanostructured patterns were distributed over the designed area precisely on a 4 inch sized wafer. Moreover, it is possible to control the size, shape, position and density of the nanostructure array through employment of the proposed

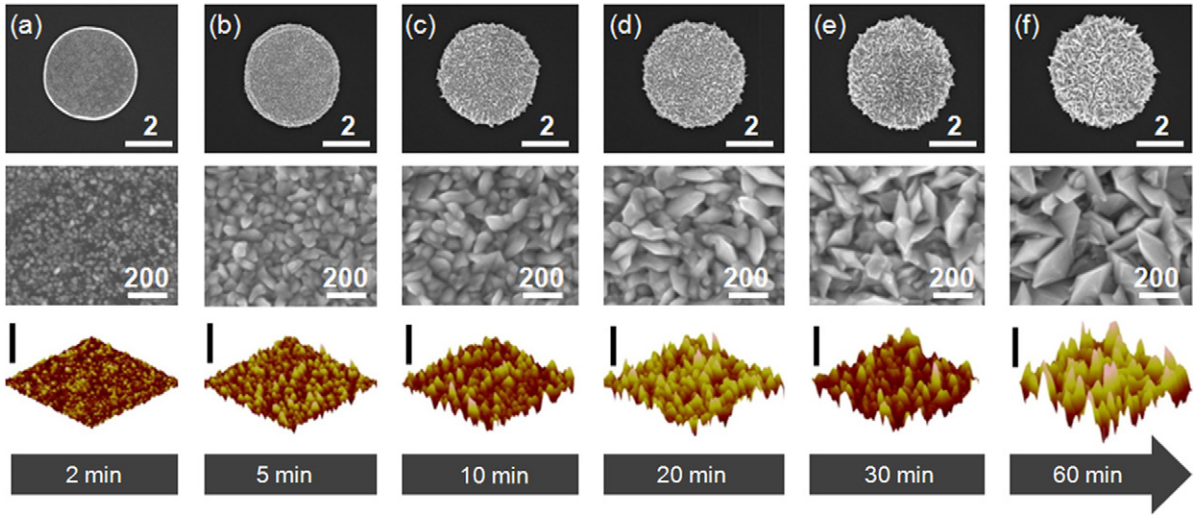

Figure 2. Representative SEM and AFM images of the Au nanocomplex with various deposition times and roughnesses: (a) deposition time of 2 min and surface mean roughness of 5.12 nm, (b) 5 min and 12.93 nm, (c) 10 min and 20.49 nm, (d) 20 min and 24.15 nm, (e) 30 min and 28.79 nm, and (f) 60 min and 49.58 nm. The SEM scale bar is in μm in the first row and in nm in the second row. For AFM images, the scanned area is 2×2 μm^2 and the height scale bar is 200 nm.

combinational process. The controllability of the size, shape and position becomes a considerable advantage in terms of integration and manufacturing when micro-to-nano transscale structures are implemented into a total analysis system (TAS).

The flower-like Au nanostructure, an Au nanocomplex in short, was grown in this manner on pre-patterned Au with its morphology governed by the amount of electrodeposition time. The deposition time dependence of the Au nanocomplex is illustrated by the SEM and by an atomic force microscope (AFM), as shown in figure 2. A distinctive change in the initial Au patterns was observed after 2 min of synthesis (figure 2(a)). Subsequently, dot-shaped nanoparticles commenced crystallization to form leaf-like nanoflakes, with their size and sharpness increasing. After 60 min, the Au nanocomplex transformed into a flower-like geometry, as shown in figure 2(f). During the nanostructure synthesis from 2 to 60 min, the mean surface roughness of the Au nanocomplex increased from 5.12 to 49.58 nm, as revealed by the AFM analysis.

The measured SERS intensities on Au nanocomplexes of various roughnesses depend on the surface morphology of the nanocomplex, as determined by the deposition time. Figure 3(a) illustrates the typical SERS spectra of BCB on Au nanocomplexes created with different deposition times. All SERS experiments were carried out using a micro-Raman system and the samples were excited by 300 μW of a 633 nm He–Ne laser. The dot-like Au template after 2 min of synthesis exhibits a very low SERS signal. As the deposition time increased, the SERS peaks for the BCB start to appear clearly at 586 cm^{-1}. Furthermore, the flower-like Au nanocomplex fabricated by 60 min of deposition distinctively enhanced the Raman peaks at 586, 1160 and 1420 cm^{-1}. The SERS intensity of the 586 cm^{-1} Raman band on the flower-like Au template (60 min) shows a 29-fold increase compared to that of the dot-like template (2 min of deposition). This result suggests that a longer deposition time makes the surface of the Au nanocomplex rougher, thereby improving the SERS enhancement. This is confirmed clearly by the surface morphology data shown in the AFM images of figure 2. Additionally, the longer time of deposition can make a larger amount of adsorption sites and surface area as well as higher surface roughness. Due to the increase of adsorption sites and active area, SERS intensity should be enhanced as our results have shown. However, this increment of surface area is not the only factor to enhance the SERS intensity since there is also an electromagnetic field enhancement on the sharp tips and valleys which is made by the flower-like Au nanostructure. To prove the effect of field enhancement on the sharp tips and valleys, we compared the surface area of the 2 min sample (shortest deposition time) and the 60 min sample (longest deposition time) by simple calculation from the cyclic voltammetry (CV) curve. The CV curve was measured by a commercially available potentiostat (three-electrode system). As a result, the surface area of the 60 min sample was shown to be 11 times larger than that of the 2 min sample. As shown in figure 4, however, the SERS intensity of the 586 cm^{-1} Raman band of the 60 min sample was 29 times higher than that of the 2 min sample. In conclusion, the corresponding increase in the surface area is not as large as the SERS intensity increase, and we think that the relatively higher SERS enhancement effect than the surface area effect is attributed to the field enhancement effect of the geometrical property of the flower-like Au nanostructure. Figure 4 shows that both the mean roughness and the SERS intensity on the Au nanocomplex increase as the electrodeposition time increases. Here, the increment rates of the mean roughness and SERS intensity become saturated after 10 min of deposition. This indicates that neither the surface roughness of the Au nanocomplex nor the SERS signal can be increased infinitely by simply extending the deposition time.

In order to guarantee the reliability of the Au nanocomplex template as a good SERS substrate, we tested the signal

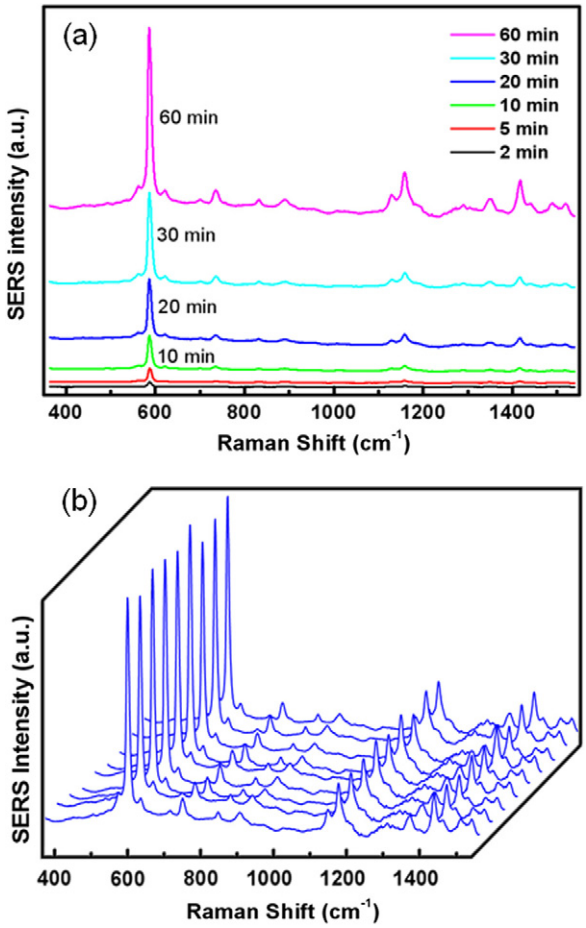

Figure 3. (a) SERS spectra of BCB molecules on an Au nanocomplex with various deposition times ranging from 2 to 60 min. The strongest Raman signal is observed at 60 min of deposition time onto an Au nanocomplex. (b) Reproducibility test for 60 min deposited Au nanocomplex. Nine Au nanocomplexes were randomly selected to measure the SERS intensity.

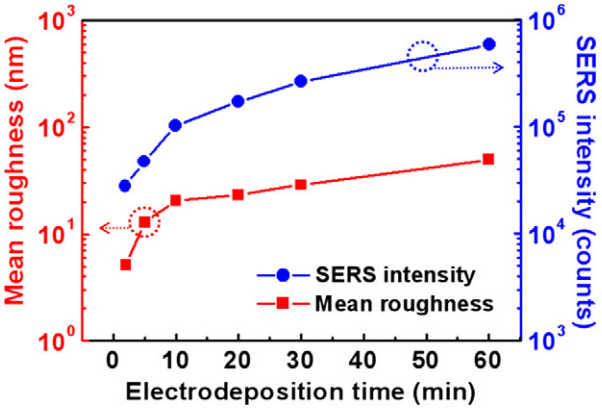

Figure 4. The relationship of the electrodeposition time, surface roughness and SERS intensity on the Au nanocomplex: a longer deposition time led to a rougher surface morphology and greater SERS intensity.

reproducibility using different Au nanocomplexes since reproducibility and stability of SERS signals from a SERS-active substrate are highly important properties for an optimum

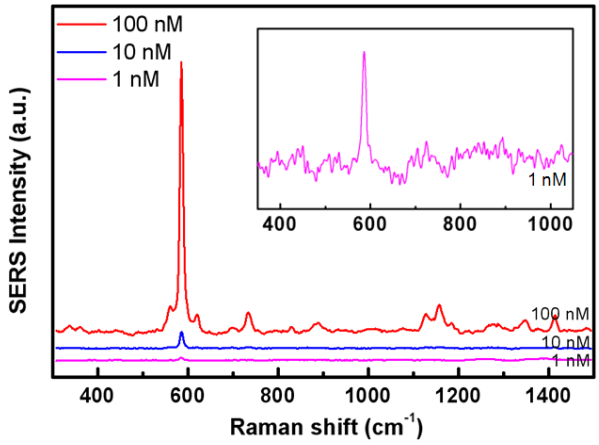

Figure 5. SERS spectra on the Au nanocomplex for inspection of the detection limit of BCB molecules: the inset shows a close-up view of the 10^{-9} M spectrum in the range of 350–1050 cm^{-1}.

sensor. Figure 3(b) shows the SERS spectra of BCB taken at nine different Au nanocomplexes, indicating high SERS signal reproducibility of the Au nanocomplexes. Some of the intensity fluctuations may be ascribed to variations in the adsorption of molecules since the BCB solution was drop-coated on Au nanocomplexes. However, the SERS signals are quite stable, demonstrating a good SERS substrate due to the controllability of the proposed combination technique.

A detection limit was also investigated using BCB molecules. 20 μl of the BCB solution at various concentrations was drop-coated on an Au nanocomplex. The starting concentration was 10^{-7} M, and this was decreased to 10^{-9} M, as shown in figure 5. As the concentration was reduced, the SERS intensity decreased continuously. The Raman band at 586 cm^{-1}, however, was observed even at the lowest concentration of 10^{-9} M (inset of figure 5). If a uniform coverage is assumed, there were approximately 11 BCB molecules in the area illuminated by the laser with a diameter of 500 nm.

Figure 6(a) shows the SERS spectrum of BT on an Au nanocomplex. The sample was incubated in 1 mM of an ethanolic solution of BT for 24 h and was then rinsed of excess solvent. The strong SERS spectrum characteristics of BT were observed. The strong SERS signals on the Au nanocomplex can be explained in terms of the geometry. The strong enhancement of the Raman signal is typically attributed to 'hot spots' that can be generated at the junction between metal surfaces upon irradiation with light. Given that Au nanocomplexes contain many interstitials, the optical fields are greatly increased, leading to a strongly enhanced Raman signal. This enhancement mechanism is directly related to the geometric control of an Au nanocomplex. The observed SERS intensity is strongly dependent on the roughness of the Au nanocomplex (figure 4). The considerable enhancement suggests that these Au nanocomplexes can serve as robust substrates capable of molecular sensing with high sensitivity. For further applications of the Au nanocomplex in the field of biomolecule detection, this study demonstrates the capability of the Au nanocomplex for the detection of adenine. Adenine

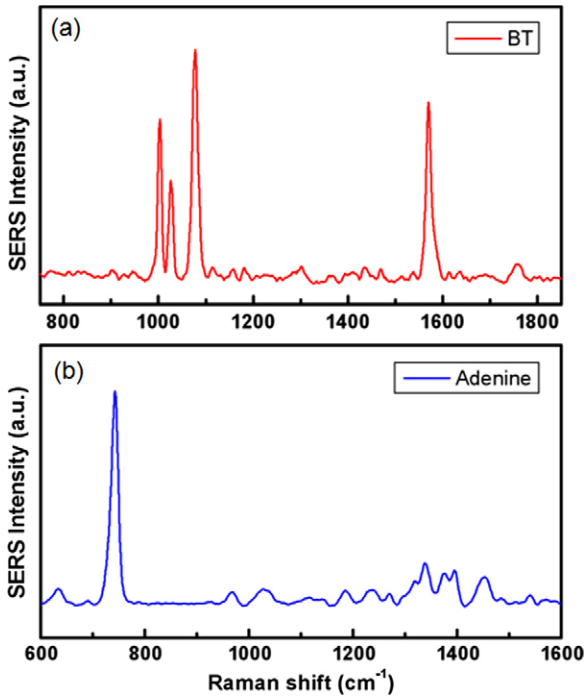

Figure 6. SERS spectra of (a) BT and (b) adenine from an Au nanocomplex array: all experiments were carried out using an Au nanocomplex formed with a deposition time of 60 min (figure 2(f)).

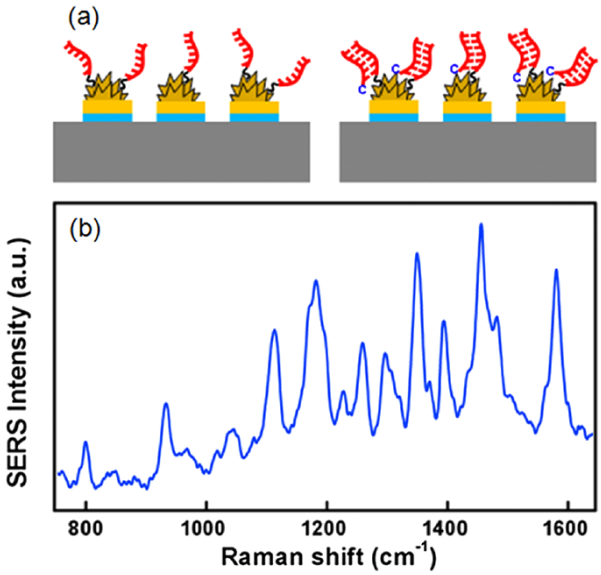

Figure 7. Demonstration of biomolecule sensing. (a) Schematic of DNA immobilization and hybridization on the Au nanocomplex array. (b) SERS spectra of Cy5 from target ssDNA attached on the Au nanocomplex array: all experiments were carried out using an Au nanocomplex formed with a deposition time of 60 min (figure 2(f)).

is one of the building blocks of DNA which is considered as an important biomolecule to be researched with proteins. 20 μl of 1 μM adenine solution was dropped and dried onto an Au nanocomplex. Figure 6(b) shows the SERS spectrum of the adenine, which clearly displays Raman bands at 740, 1330 and 1450 cm^{-1}. This indicates that the Au nanocomplex can be utilized for the detection of biomolecules at low concentrations.

For the demonstration of biomolecule sensing, we have additionally tried the detection of single-stranded DNA using this sensor. Figure 7(a) shows the schematic of Au nanocomplexes before (left) and after (right) hybridization of a target single-stranded DNA. A 20-mer oligonucleotide was used as a model target strand and Cy5 was modified at the end of the target for the Raman signal. Details of the experimental method are as follows. The thiol-terminated probe DNA (5′-AGTACCGTGAGGGAAAGGCG-SH-3′, purchased from Genotech in Daejeon, Korea) was treated with 1 M dithiothreitol (DTT) to reduce the disulfide bond and was purified using a NAP-5 column (GE Healthcare Co.). The 10 μM probe DNA in 1 M KH_2PO_4 (pH 6.75) was immobilized on the surface of the gold flower chips at room temperature for 24 h. After incubation, excessive DNA was washed with 0.2% (v/v) sodium dodecyl sulfate (SDS) for 5 min. The 1 μM target DNA in the phosphate buffered saline (PBS) solution (5′-Cy5-CGCCTTTCCCTCACGGTACT − 3′) which is complementary to the probe DNA was hybridized at 30 °C for 6 h. After washing with PBS solution containing 0.1% (v/v) SDS for 5 min, the SERS signal on the Au nanocomplexes was measured. The Au nanocomplexes were functionalized with the complement of the target sequence and incubated with the target strand, so as to capture the targets through sequence-selective hybridization on Au nanocomplexes. A strong SERS signal is observed after hybridization (figure 7(b)) and a featureless spectrum is obtained when a noncomplementary target DNA strand was used. This means there is the possibility of DNA detection by well-ordered Au nanocomplexes after further optimizations.

4. Conclusions

In summary, this study describes the development of a well-ordered and integrated Au nanostructure on a large-scale substrate as a SERS template combining both a top-down lithography and a bottom-up electrodeposition technique. The correlation of the length of the electrodeposition time in the fabrication of the Au nanostructure with the SERS enhancement was analyzed. High-quality SERS spectra were obtained for various molecules. This Au nanocomplex array and its strong SERS enhancement can be implemented on a lab-on-a-chip-based total analysis system for label-free chemical and biomolecular detection processes.

Acknowledgments

This work was supported by the NRL Program of the Korea Science and Engineering Foundation (KOSEF) grant funded by the Korean Government (MEST) (ROA-2007-000-20028-0 and ROA-2007-000-20127-0).

References

[1] Li Y and Shi G 2005 *J. Phys. Chem.* B **109** 23787
[2] Qian L and Yang X 2005 *J. Phys. Chem.* B **110** 16672

[3] He Y, Yu X and Yang B 2006 *Mater. Chem. Phys.* **99** 295
[4] Li Y, Lu G and Shi G 2006 *J. Phys. Chem.* B **110** 24585
[5] Guieu V, Langugne-Labarthet F, Servant L, Talaga D and Sojic N 2008 *Small* **4** 96
[6] Bhuvana T, Kumar G V P, Kulkarni G U and Narayana C 2007 *J. Phys. Chem.* C **111** 6700
[7] Duan G, Cai W, Luo Y, Li Z and Li Y 2006 *Appl. Phys. Lett.* **89** 211905
[8] Qian L H, Yan X Q, Fujita T, Inoue A and Chen M W 2007 *Appl. Phys. Lett.* **90** 153120
[9] Shanmukh S, Jones L, Driskell J, Zhao Y, Dluhy R and Tripp R A 2006 *Nano Lett.* **6** 2630
[10] Alvarez-Puebla R, Cui B, Bravo-Vasquez J, Veres T and Fenniri H 2007 *J. Phys. Chem.* C **111** 6720
[11] Liu G L and Lee L P 2005 *Appl. Phys. Lett.* **87** 074101
[12] Mohanty P *et al* 2007 *J. Am. Chem. Soc.* **129** 9576
[13] Knelpp J, Knelpp H, McLaughlin M, Brown D and Knelpp K 2006 *Nano Lett.* **6** 2225
[14] Sackmann M, Bom S, Balster T and Materny A 2006 *J. Raman Spectrosc.* **38** 277
[15] Whitney A V, Elam J W, Stair P C and Van Duyne R P 2007 *J. Phys. Chem.* C **111** 16827
[16] Sun L, Song Y, Wang L, Guo C, Sun Y, Liu Z and Li Z 2008 *J. Phys. Chem.* C **112** 1415
[17] Li Z, Tong W M, Stickle W F, Neiman D L and Williams R S 2007 *Langmuir* **23** 5135
[18] Zhang X, Zhao J, Whitney A V, Elam J W and Van Duyne R P 2006 *J. Am. Chem. Soc.* **128** 10304
[19] Kim J-H, Huang X-J and Choi Y-K 2008 *J. Phys. Chem.* C **112** 12747